

## Evaluation of the Shielding Properties of Various Water Equivalent Materials Using Different Calculation Methods and Monte Carlo

Turan ŞAHMARAN<sup>1\*</sup>

<sup>1</sup>Hatay Mustafa Kemal University, Kırıkhan Vocational School, Hatay, Turkey  
(ORCID: [0000-0003-3708-6162](https://orcid.org/0000-0003-3708-6162))



**Keywords:** Radiation Shielding, Monte Carlo, Water Equivalent Materials, Effective Removal Cross Sections

### Abstract

In this study, linear attenuation coefficients (LAC), mass attenuation coefficients (MAC), half-valued layer (HVL), and mean free path (MFP) values of various materials such as water equivalent, ABS, Presage, RMI<sub>457</sub>, RW<sub>3</sub>, SW<sub>557</sub>, Epoxy, A<sub>150</sub>, Rhizophora spp., and Nylon-12 were found. These values were calculated using Monte Carlo simulation, EpiXS, Phy-X/PSD, and XCOM programs. Additionally, the fast neutron effective removal cross sections ( $\Sigma R$ ) have been calculated using the empirical calculation method, Phy-X/PSD, MRCsC program, experimental, and MNCP5 with the help of fast neutron mass removal cross sections. Among all the materials studied, Nylon-12 has the highest  $\Sigma R$  value. The calculated values of HVL, MFP, LAC, and MAC reveal that RW<sub>3</sub>, Epoxy, and Presage are the best materials in terms of their shielding properties, respectively.

## 1. Introduction

In radiation protection, the evaluation of various interaction parameters such as mass attenuation coefficient ( $\mu/\rho$ ), half-value layer (HVL), mean free path (MFP), and total interaction cross-section ( $\sigma_t$ ) is crucial for practical applications of protective materials in radiation dosimetry, nuclear medicine, radiation therapy, and radiology fields. Lead and concrete-based materials are currently the most commonly used materials for protecting against X-ray, gamma-ray, and neutron radiation in radiation fields. However, researchers in the field of radiation protective materials are actively seeking alternative material designs due to the environmental toxicity and harmful effects on human health associated with lead (Pb). Furthermore, lead exhibits a blind absorption region for X-rays in the range of 70-90 keV, which has led to the exploration of various alternative materials [1]. Not only X-rays or gamma rays but also radiation from neutrons

have led to the design of many new protective materials. Neutron radiation has been used in various fields for many years, such as cancer treatments, the production of radioisotopes, industrial radiography, and the characterization of various materials [2, 3]. However, the use and production of free neutrons entail certain risks. Among these risks, free neutrons can alter the microstructural properties of materials and indirectly cause double-strand breaks in the DNA molecule of biological matter. This can lead to cell mutations and death [4, 5]. Therefore, the shielding design for neutrons is one of the important considerations in radiation safety [6, 7]. In recent years, the shielding properties of many new materials or different materials with modified characteristics have been investigated [8, 9]. For effective neutron radiation shielding, the material structure should consist of hydrogen-rich or low atomic number element combinations [10]. One of the fundamental

\*Corresponding author: [tsahmaran@gmail.com](mailto:tsahmaran@gmail.com)

Received: 22.07.2023, Accepted: 12.03.2024

quantities used for predicting neutron shielding is the fast neutron effective removal cross-section ( $\Sigma R$ ) [11]. This empirical cross-section has been derived for hydrogenous systems and utilized in reactor shielding calculation methods. Researchers use experimental measurements, theoretical models, and nuclear data libraries to determine and predict HVL, MFP, MAC, LAC, and fast neutron removal cross-sections for different materials and energy ranges. These data sources are continuously updated and improved to enhance the accuracy of cross-section values and ensure the reliability of nuclear calculations and simulations. The interaction of neutrons with matter is described by parameters such as  $\Sigma R$ ,

## 2. Material and Method

### 2.1 Theory

The initial intensity of a monoenergetic photon is  $I_0$ . The intensity of the photon beam ( $I$  is the attenuated photon intensities) passing through the attenuating thickness ( $x$ , cm) will decrease. The attenuation of the photon beam is determined using Equation 1, with the help of the Beer-Lambert law [12].

$$I = I_0^{-\mu x} \quad (1)$$

Here,  $\mu$  ( $\text{cm}^{-1}$ ) represents the LAC. The MAC value for the compound and mixture is defined using Equation 2 [13].

$$\mu_m = \frac{\mu}{\rho} = \sum w_i \left( \frac{\mu_i}{\rho_i} \right) \quad (2)$$

Here,  $\mu_m$  ( $\text{cm}^2/\text{g}$ ) represents the MAC.  $w_i$  represents the weight fraction of the  $i$ th element in the material, and  $\rho$  ( $\text{g}/\text{cm}^3$ ) represents the density of the shielding material. The parameter  $\mu$  is important for calculating the values that will reduce the initial value of primary radiation to half or one-tenth [14, 15]. MFP represents the average distance traveled by photons before interacting with the absorbing material. Equation 3 provides the formulas for HVL and MFP.

$$HVL = \frac{\ln 2}{\mu}, \text{MFP} = \frac{1}{\mu} \quad (3)$$

Equations 4, 5, and 6 present the calculations related to materials and neutrons.  $\Sigma R$  represents the probability of neutrons passing through the material without interaction. An empirical approach model was derived for the mass removal cross-section ( $\Sigma_R/\rho$ ) [16].

MFP, and HVL, among others.  $\Sigma R$  is known as a characteristic of materials. To predict the  $\Sigma R$  of any material, a dataset of elemental mass removal cross-sections ( $\Sigma_R/\rho$ ) is used [11]. This research involved computing the LAC, MAC, HVL, and MFP measurements for different substances like ABS, presage, RMI<sub>457</sub>, RW<sub>3</sub>, SW<sub>557</sub>, epoxy, A<sub>150</sub>, Rhizophora spp. (Rspp), and Nylon-12 within a photon energy span of 0.1-18 MeV. Furthermore, the  $\Sigma R$  values for these materials were assessed using MRCsC, Phy-X/PSD, Monte Carlo N-Particle Transport Code (MCNP5), and empirical calculation approaches.

$$\Sigma R = \sum_i \rho_i (\Sigma_{R/\rho})_i \quad (4)$$

$$\rho_i = \sum_s w_i \rho_s \quad (5)$$

$$\Sigma_{R/\rho} = 0.190 Z^{-0.743} \quad Z \leq 8$$

$$\text{and } \Sigma_{R/\rho} = 0.125 Z^{-0.565} \quad Z > 8 \quad (6)$$

Here,  $\rho_i$  represents the partial density,  $(\Sigma_{R/\rho})_i$  represents the mass removal cross-section of the  $i$ th component,  $w_i$  is the weight fraction of the constituent,  $\rho_s$  is the sample density,  $A$  is the atomic weight, and  $Z$  is the atomic number.

### 2.2 GATE Simulation, MRCsC, EpiXS, and Phy-X/PSD program

The simulation program vGate, version 8.1, was utilized. GATE is an advanced opensource software developed by the international OpenGATE collaboration. All materials used were defined by entering their densities and mass ratios into the *gate.material.db* file. The geometry was designed with a distance of 100 cm between the source and the detector. Initially, with no material present, the simulation was run to obtain the  $I_0$  value. Subsequently, by placing a material with dimensions of  $10 \times 10 \times 10 \text{ cm}^3$  between the source and the detector, the  $I$  value was obtained. To determine the  $I_0$  and  $I$  values, a fluence actor was defined in the GATE macro file. This actor counts the fraction of a particle that passes through a volume. MRCsC has been developed to accurately and precisely predict the macroscopic effective removal cross-section,  $\Sigma R$ , for fast neutrons in various shielding materials. The program incorporates the latest data published by the Evaluated Nuclear Data Library 'ENDF/BVIII' [17]. EpiXS is a Windows-based program used for photon

attenuation, dosimetry, and shielding. It includes the EPICS2017 (ENDF/B-VIII) and EPDL97 (ENDF/B-VI.8) data libraries [18]. Phy-X/PSD is the software program of an online tool used for calculating parameters related to radiation shielding and dosimetry [19]. Figure 1 shows the simulation geometry.

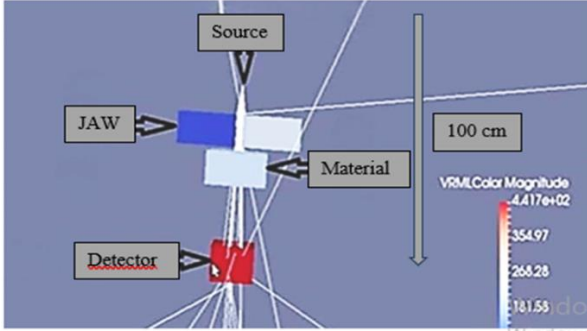


Figure 1. Simulation geometry (not scale)

### 3. Results and Discussion

In radiotherapy, especially during daily, weekly, or monthly quality control procedures, water-equivalent phantom materials are commonly used. In this study, various photon energies were investigated for the MAC, LAC, HVL, and MFP values of these materials. For these calculations, GATE, EpiXS, and XCOM were respectively employed as simulation, computer program, and theoretical calculation tools. Furthermore, the  $\Sigma_R$  values of these materials were obtained using empirical formulas, MRCsC, Phy-X/PSD, and MNCP5 by utilizing the  $\Sigma_R/\rho$  values found. Table 1 illustrates the elemental composition of the materials used.

Table 1. Density ( $\rho$ , g cm<sup>-3</sup>) and elemental composition of the phantom material

	RW <sub>3</sub> <sup>[20]</sup>	SW <sub>557</sub> <sup>[21]</sup>	ABS <sup>[22]</sup>	Epoxy <sup>[23]</sup>	Presage <sup>[24]</sup>	RMI <sub>457</sub> <sup>[21]</sup>	Nylon <sub>12</sub> <sup>[20]</sup>	A <sub>150</sub> <sup>[25]</sup>	Rsp <sup>[26]</sup>
H	0.075	0.081	0.081	0.064	0.089	0.080	0.117	0.101	
C	0.904	0.657	0.852	0.642	0.607	0.672	0.730	0.775	0.515
N		0.022	0.066		0.044	0.024	0.070	0.035	
O	0.008	0.193		0.203	0.217	0.199	0.081	0.052	0.422
B		0.001							
F								0.017	0.062
Cl		0.001		0.090	0.033	0.001			
Ca		0.018				0.023		0.018	
Na		0.002							
Mg		0.010							
Al		0.001							
Si		0.011							
S		0.001							
Ti	0.012								
Br					0.008				
$\rho$	1.045	1.032	1.040	1.110	1.101	1.030	1.010	1.127	1.030

Tables 2 and 3 show that, due to the photoelectric effect, decreases in MAC and LAC values are more pronounced at lower energies compared to higher energies. The reason for this sharp decrease is attributed to the photoelectric cross-section being associated with  $Z^{4-5}$  and  $E^{-3.5}$  in the low-energy region. As shown in Tables 2 and 3, the data obtained between 0.8 MeV and 10 MeV energies indicate that MAC and LAC values are almost the same for all materials. In these energy ranges, the probability of the photoelectric effect is low, as the photon energy is higher than the energy required for electron

transitions. Another significant interaction process known as Compton scattering becomes more dominant in this range, and in this case, the cross-section is proportional to  $E^{-1}$  and  $Z$ . After Compton scattering, the pair production process starts to dominate, and this process is proportional to  $Z^2$  in terms of cross-section. As the energy increases, it can be observed that the MAC and LAC values decrease. In Tables 2 and 3, the highest MAC and LAC values were observed in the RW3 material at 0.01 MeV. The RW<sub>3</sub> (29.254 cm<sup>2</sup> g<sup>-1</sup>) material exhibits a sudden

change in MAC values around absorption edges due to its high Z (Ti) content.

**Table 2.** The MAC values of materials were compared with the GATE, EpiXS, and XCOM

Energy (MeV)	0.01	0.05	0.08	0.1	0.5	0.8	1	3	6	10	15	18
<b>GATE</b> RW <sub>3</sub>	29.254	0.425	0.229	0.178	0.088	0.070	0.063	0.036	0.024	0.021	0.017	0.016
<b>XCOM</b> RW <sub>3</sub>	31.090	0.465	0.232	0.189	0.089	0.072	0.065	0.037	0.026	0.022	0.020	0.019
<b>EpiXS</b> RW <sub>3</sub>	31.136	0.466	0.232	0.190	0.090	0.072	0.065	0.037	0.027	0.022	0.020	0.020
<b>GATE</b> SW <sub>557</sub>	4.975	0.219	0.171	0.160	0.090	0.072	0.065	0.035	0.021	0.019	0.017	0.015
<b>XCOM</b> SW <sub>557</sub>	5.258	0.224	0.179	0.166	0.094	0.076	0.068	0.038	0.026	0.021	0.018	0.017
<b>EpiXS</b> SW <sub>557</sub>	5.263	0.225	0.179	0.166	0.094	0.076	0.069	0.038	0.027	0.021	0.018	0.017
<b>GATE</b> ABS	2.146	0.191	0.168	0.165	0.091	0.071	0.060	0.032	0.023	0.020	0.016	0.014
<b>XCOM</b> ABS	2.312	0.199	0.173	0.163	0.094	0.076	0.068	0.038	0.026	0.021	0.018	0.017
<b>EpiXS</b> ABS	2.315	0.200	0.173	0.163	0.094	0.076	0.069	0.038	0.026	0.021	0.018	0.015
<b>GATE</b> Epoxy	7.911	0.238	0.175	0.160	0.086	0.070	0.062	0.030	0.023	0.019	0.016	0.015
<b>XCOM</b> Epoxy	7.927	0.243	0.181	0.166	0.092	0.075	0.067	0.037	0.026	0.021	0.018	0.017
<b>EpiXS</b> Epoxy	7.934	0.244	0.182	0.166	0.092	0.075	0.067	0.038	0.026	0.021	0.019	0.018
<b>GATE</b> Presage	5.138	0.250	0.179	0.165	0.090	0.069	0.065	0.033	0.022	0.018	0.017	0.018
<b>XCOM</b> Presage	5.273	0.256	0.188	0.171	0.094	0.076	0.069	0.038	0.026	0.021	0.018	0.018
<b>EpiXS</b> Presage	5.276	0.256	0.188	0.171	0.095	0.077	0.069	0.039	0.027	0.021	0.019	0.017
<b>GATE</b> RMI <sub>457</sub>	4.983	0.213	0.172	0.162	0.092	0.071	0.063	0.038	0.024	0.020	0.017	0.015
<b>XCOM</b> RMI <sub>457</sub>	5.065	0.223	0.179	0.166	0.094	0.076	0.068	0.038	0.026	0.021	0.018	0.017
<b>EpiXS</b> RMI <sub>457</sub>	5.071	0.224	0.179	0.166	0.094	0.076	0.069	0.038	0.027	0.021	0.018	0.017
<b>GATE</b> Nylon <sub>12</sub>	2.519	0.201	0.171	0.160	0.092	0.070	0.066	0.034	0.022	0.019	0.016	0.015
<b>XCOM</b> Nylon <sub>12</sub>	2.537	0.207	0.179	0.168	0.097	0.079	0.070	0.039	0.027	0.021	0.017	0.018
<b>EpiXS</b> Nylon <sub>12</sub>	2.540	0.207	0.179	0.169	0.097	0.079	0.071	0.040	0.027	0.021	0.018	0.017
<b>GATE</b> A <sub>150</sub>	4.149	0.215	0.175	0.163	0.091	0.072	0.064	0.032	0.022	0.020	0.018	0.016
<b>XCOM</b> A <sub>150</sub>	4.146	0.219	0.180	0.167	0.095	0.077	0.069	0.039	0.026	0.021	0.018	0.017
<b>EpiXS</b> A <sub>150</sub>	4.151	0.219	0.181	0.168	0.096	0.078	0.070	0.039	0.027	0.021	0.018	0.017
<b>GATE</b> R <sub>spp</sub>	4.299	0.211	0.162	0.151	0.080	0.065	0.061	0.033	0.026	0.018	0.016	0.014
<b>XCOM</b> R <sub>spp</sub>	4.250	0.200	0.164	0.152	0.086	0.070	0.063	0.036	0.025	0.020	0.017	0.017
<b>EpiXS</b> R <sub>spp</sub>	4.253	0.200	0.164	0.153	0.087	0.071	0.063	0.036	0.025	0.020	0.018	0.017

**Table 3.** The LAC values of materials were compared with the GATE, EpiXS, and XCOM

Energy (MeV)	0.01	0.05	0.08	0.1	0.5	0.8	1	3	6	10	15	18
<b>GATE</b> RW <sub>3</sub>	30.570	0.444	0.239	0.186	0.092	0.073	0.066	0.038	0.025	0.022	0.018	0.017
<b>XCOM</b> RW <sub>3</sub>	32.480	0.485	0.242	0.197	0.093	0.075	0.067	0.038	0.027	0.022	0.020	0.019
<b>EpiXS</b> RW <sub>3</sub>	32.537	0.487	0.243	0.198	0.094	0.076	0.068	0.039	0.028	0.023	0.021	0.021
<b>GATE</b> SW <sub>557</sub>	5.134	0.226	0.176	0.165	0.093	0.074	0.067	0.036	0.022	0.020	0.018	0.015
<b>XCOM</b> SW <sub>557</sub>	5.426	0.231	0.184	0.171	0.097	0.078	0.070	0.039	0.026	0.021	0.018	0.017
<b>EpiXS</b> SW <sub>557</sub>	5.432	0.232	0.185	0.172	0.097	0.079	0.071	0.040	0.027	0.022	0.019	0.018
<b>GATE</b> ABS	2.232	0.199	0.175	0.172	0.095	0.074	0.062	0.033	0.024	0.021	0.017	0.015

<b>XCOM_ABS</b>	2.404	0.207	0.180	0.170	0.098	0.079	0.071	0.040	0.027	0.022	0.019	0.018
<b>EpiXS_ABS</b>	2.408	0.208	0.180	0.170	0.098	0.079	0.071	0.040	0.027	0.021	0.018	0.017
<b>GATE_Epoxy</b>	8.781	0.264	0.194	0.178	0.095	0.078	0.069	0.033	0.026	0.021	0.018	0.017
<b>XCOM_Epoxy</b>	8.799	0.270	0.201	0.184	0.102	0.083	0.074	0.041	0.029	0.023	0.020	0.019
<b>EpiXS_Epoxy</b>	8.807	0.271	0.202	0.184	0.103	0.083	0.075	0.042	0.029	0.023	0.021	0.020
<b>GATE_Presage</b>	5.657	0.275	0.197	0.182	0.099	0.076	0.072	0.036	0.024	0.020	0.019	0.020
<b>XCOM_Presage</b>	5.806	0.282	0.207	0.188	0.103	0.085	0.076	0.043	0.030	0.023	0.021	0.017
<b>EpiXS_Presage</b>	5.809	0.282	0.207	0.189	0.104	0.085	0.076	0.043	0.030	0.023	0.020	0.019
<b>GATE_RMI<sub>457</sub></b>	5.132	0.219	0.177	0.167	0.095	0.073	0.065	0.039	0.025	0.021	0.018	0.015
<b>XCOM_RMI<sub>457</sub></b>	5.217	0.230	0.184	0.171	0.097	0.078	0.070	0.039	0.027	0.022	0.019	0.018
<b>EpiXS_RMI<sub>457</sub></b>	5.223	0.231	0.184	0.171	0.097	0.079	0.071	0.040	0.027	0.022	0.019	0.018
<b>GATE_Nylon<sub>12</sub></b>	2.544	0.203	0.173	0.162	0.093	0.071	0.067	0.034	0.022	0.019	0.016	0.015
<b>XCOM_Nylon<sub>12</sub></b>	2.562	0.209	0.181	0.170	0.098	0.080	0.071	0.039	0.027	0.021	0.017	0.018
<b>EpiXS_Nylon<sub>12</sub></b>	2.565	0.210	0.181	0.170	0.098	0.080	0.072	0.040	0.027	0.021	0.018	0.017
<b>GATE_A<sub>150</sub></b>	4.676	0.242	0.197	0.184	0.103	0.081	0.072	0.036	0.025	0.023	0.020	0.018
<b>XCOM_A<sub>150</sub></b>	4.673	0.247	0.203	0.188	0.107	0.087	0.078	0.044	0.029	0.024	0.020	0.019
<b>EpiXS_A<sub>150</sub></b>	4.678	0.247	0.202	0.189	0.107	0.088	0.079	0.044	0.034	0.023	0.021	0.019
<b>GATE_Rspp</b>	4.428	0.217	0.167	0.156	0.082	0.067	0.063	0.034	0.027	0.019	0.016	0.014
<b>XCOM_Rspp</b>	4.378	0.206	0.169	0.157	0.089	0.072	0.065	0.037	0.026	0.021	0.018	0.018
<b>EpiXS_Rspp</b>	4.381	0.203	0.167	0.154	0.087	0.073	0.064	0.035	0.024	0.022	0.017	0.016

HVL and MFP characterize the photon attenuation performance of the materials (Tables 4 and 5). A low HVL and MFP values represent the need for a thinner material to absorb photons. The density of the material is inversely proportional to the HVL and MFP values. The presence of low Z elements (H, C, N, and O) within the material ensures higher HVL and MFP values are achieved. For a sample to be considered a shielding material, it is required to have maximum MAC and minimum HVL and MFP values within the selected range of photon energies. According to Table 4, the RW<sub>3</sub> (0.023 cm) material has a lower HVL value compared to the other

materials. Following the RW<sub>3</sub> material, epoxy (0.079 cm) and presage (0.123 cm) exhibit the best shielding properties, respectively. According to Table 4, it is observed that as the photon energy increases, the HVL value also increases. MFP is defined as the average distance a photon can travel in the target material before interacting with its atoms. According to Table 5, among the investigated materials, RW<sub>3</sub> (0.033 cm), epoxy (0.114 cm), and presage (0.177 cm) were found to have the lowest MFP values, respectively. Figure 2 shows HVL values according to energy variation.

**Table 4.** The HVL values of materials were compared with the GATE, EpiXS, and XCOM

Energy (MeV)	0.01	0.05	0.08	0.1	0.5	0.8	1	3	6	10	15	18
<b>GATE RW<sub>3</sub></b>	0.023	1.560	2.896	3.726	7.536	9.474	10.526	18.421	27.632	31.579	39.009	41.447
<b>XCOM RW<sub>3</sub></b>	0.021	1.426	2.858	3.509	7.451	9.211	10.202	17.923	25.506	30.144	33.158	34.903
<b>EpiXS RW<sub>3</sub></b>	0.021	1.422	2.853	3.493	7.410	9.152	10.191	17.948	24.845	27.700	32.575	33.452
<b>GATE SW<sub>557</sub></b>	0.135	3.066	3.927	4.197	7.461	9.327	10.331	19.186	31.977	35.343	39.501	44.767
<b>XCOM SW<sub>557</sub></b>	0.128	2.998	3.751	4.045	7.144	8.836	9.875	17.671	25.827	31.977	37.306	39.501
<b>EpiXS SW<sub>557</sub></b>	0.128	2.895	3.744	4.039	7.138	8.792	9.783	17.484	25.240	31.794	36.681	38.560
<b>GATE ABS</b>	0.311	3.489	3.966	4.038	7.322	9.385	11.106	20.823	28.972	33.317	41.647	47.596
<b>XCOM ABS</b>	0.288	3.348	3.852	4.088	7.089	8.768	9.799	17.535	25.629	31.731	37.019	39.197

<b>EpiXS_ABS</b>	0.285	3.334	3.849	4.088	7.088	8.728	9.711	17.407	25.349	32.305	37.719	39.885
<b>GATE Epoxy</b>	0.079	2.623	3.568	3.902	7.260	8.919	10.070	20.811	27.145	32.859	39.020	41.622
<b>XCOM Epoxy</b>	0.079	2.569	3.449	3.761	6.786	8.324	9.318	16.874	24.012	29.730	34.685	36.725
<b>EpiXS Epoxy</b>	0.077	2.562	3.436	3.759	6.760	8.329	9.268	16.520	23.662	29.504	33.693	35.245
<b>GATE Presage</b>	0.123	2.518	3.516	3.815	6.994	9.122	9.684	19.074	28.610	34.968	37.025	34.968
<b>XCOM Presage</b>	0.119	2.459	3.348	3.681	6.696	8.196	9.109	16.264	23.486	29.551	34.023	35.763
<b>EpiXS Presage</b>	0.118	2.455	3.345	3.675	6.652	8.176	9.120	16.293	23.480	29.540	34.012	35.737
<b>GATE RMI<sub>457</sub></b>	0.135	3.159	3.912	4.153	7.313	9.476	10.680	17.706	28.034	33.641	39.577	44.854
<b>XCOM RMI<sub>457</sub></b>	0.133	3.017	3.759	4.053	7.158	8.853	9.894	17.706	25.878	32.039	37.379	39.577
<b>EpiXS RMI<sub>457</sub></b>	0.132	3.007	3.758	4.053	7.158	8.817	9.811	17.539	25.343	31.964	36.924	38.840
<b>GATE Nylon<sub>12</sub></b>	0.272	3.414	4.013	4.288	7.458	9.802	10.396	20.181	31.188	36.113	42.884	45.743
<b>XCOM Nylon<sub>12</sub></b>	0.270	3.315	3.833	4.084	7.074	8.685	9.802	17.593	25.413	32.673	40.361	38.119
<b>EpiXS Nylon<sub>12</sub></b>	0.271	3.308	3.821	4.072	7.064	8.697	9.677	17.358	25.326	32.360	37.887	40.118
<b>GATE A<sub>150</sub></b>	0.148	2.860	3.514	3.772	6.757	8.540	9.608	19.216	27.950	30.745	34.161	38.432
<b>XCOM A<sub>150</sub></b>	0.148	2.808	3.416	3.682	6.473	7.986	8.912	15.767	23.650	29.281	34.161	36.171
<b>EpiXS A<sub>150</sub></b>	0.147	2.841	3.416	3.666	6.437	7.921	8.813	15.774	22.935	29.141	33.930	35.830
<b>GATE R<sub>spp</sub></b>	0.157	3.189	4.153	4.456	8.410	10.351	11.030	20.388	25.878	37.379	42.051	48.058
<b>XCOM R<sub>spp</sub></b>	0.158	3.364	4.103	4.426	7.823	9.612	10.680	18.689	26.913	33.641	39.577	39.577
<b>EpiXS R<sub>spp</sub></b>	0.157	3.357	4.102	4.404	7.746	9.541	10.616	18.894	26.947	33.414	37.941	39.579

**Table 5.** The MFP values of materials were compared with the GATE, EpiXS, and XCOM

<b>Energy (MeV)</b>	<b>0.01</b>	<b>0.05</b>	<b>0.08</b>	<b>0.1</b>	<b>0.5</b>	<b>0.8</b>	<b>1</b>	<b>3</b>	<b>6</b>	<b>10</b>	<b>15</b>	<b>18</b>
<b>GATE RW<sub>3</sub></b>	0.033	2.252	4.179	5.376	10.874	13.671	15.189	26.582	39.872	45.568	56.290	59.809
<b>XCOM RW<sub>3</sub></b>	0.031	2.058	4.125	5.063	10.752	13.291	14.722	25.863	36.805	43.497	47.847	50.365
<b>EpiXS RW<sub>3</sub></b>	0.031	2.052	4.117	5.039	10.691	13.204	14.702	25.893	35.844	42.847	46.966	48.261
<b>GATE SW<sub>557</sub></b>	0.195	4.425	5.667	6.056	10.767	13.458	14.908	27.685	46.142	51.000	57.000	64.599
<b>XCOM SW<sub>557</sub></b>	0.184	4.326	5.413	5.837	10.308	12.750	14.250	25.500	37.269	46.142	53.833	57.000
<b>EpiXS SW<sub>557</sub></b>	0.184	4.307	5.401	5.827	10.299	12.684	14.115	25.225	36.414	4.869	52.920	55.631
<b>GATE ABS</b>	0.448	5.034	5.723	5.828	10.566	13.543	16.026	30.048	41.806	48.077	60.096	68.681
<b>XCOM ABS</b>	0.416	4.832	5.558	5.899	10.229	12.652	14.140	25.304	36.982	45.788	53.419	56.561
<b>EpiXS ABS</b>	0.415	4.81	5.553	5.898	10.226	12.591	14.01	25.113	36.571	46.607	54.417	57.542
<b>GATE Epoxy</b>	0.114	3.785	5.148	5.631	10.476	12.870	14.531	30.030	39.170	47.416	56.306	60.060
<b>XCOM Epoxy</b>	0.114	3.707	4.977	5.427	9.792	12.012	13.446	24.349	34.650	42.900	50.050	52.994
<b>EpiXS Epoxy</b>	0.114	3.695	4.958	5.423	9.753	12.016	13.372	23.833	34.137	42.566	48.608	50.848
<b>GATE Presage</b>	0.177	3.633	5.074	5.505	10.092	13.163	13.973	27.523	41.285	50.459	53.427	50.459
<b>XCOM Presage</b>	0.172	3.548	4.831	5.311	9.662	11.826	13.144	23.469	33.890	42.642	49.095	51.606
<b>EpiXS Presage</b>	0.172	3.541	4.826	5.302	9.597	11.824	13.158	23.505	33.888	42.617	49.894	51.557
<b>GATE RMI<sub>457</sub></b>	0.195	4.558	5.645	5.993	10.553	13.674	15.411	25.549	40.453	48.544	57.110	64.725
<b>XCOM RMI<sub>457</sub></b>	0.192	4.354	5.424	5.849	10.328	12.775	14.278	25.549	37.341	46.232	53.937	57.110
<b>EpiXS RMI<sub>457</sub></b>	0.191	4.338	5.424	5.848	10.327	12.72	14.154	25.303	36.562	46.114	53.27	56.034
<b>GATE Nylon<sub>12</sub></b>	0.393	4.926	5.790	6.188	10.762	14.144	15.002	29.121	45.005	52.110	61.881	66.007

<b>XCOM_Nylon12</b>	0.390	4.783	5.531	5.893	10.207	12.533	14.144	25.387	36.670	47.148	58.241	55.006
<b>EpiXS_Nylon12</b>	0.391	4.772	5.528	5.875	10.191	12.548	13.961	25.042	36.537	46.686	54.660	57.879
<b>GATE_A150</b>	0.214	4.127	5.070	5.444	9.751	12.324	13.864	27.728	40.332	44.366	49.295	55.457
<b>XCOM_A150</b>	0.214	4.052	4.930	5.313	9.340	11.524	12.860	22.752	34.127	42.253	49.295	52.195
<b>EpiXS_A150</b>	0.213	4.042	4.930	5.292	9.271	11.421	12.844	22.763	33.081	42.044	48.953	51.693
<b>GATE_Rspp</b>	0.226	4.601	5.993	6.430	12.136	14.937	15.916	29.420	37.341	53.937	60.680	69.348
<b>XCOM_Rspp</b>	0.228	4.854	5.920	6.387	11.289	13.870	15.411	26.969	38.835	48.544	57.110	57.110
<b>EpiXS_Rspp</b>	0.228	4.844	5.918	6.354	11.175	13.764	15.316	27.258	38.877	48.206	54.377	57.100

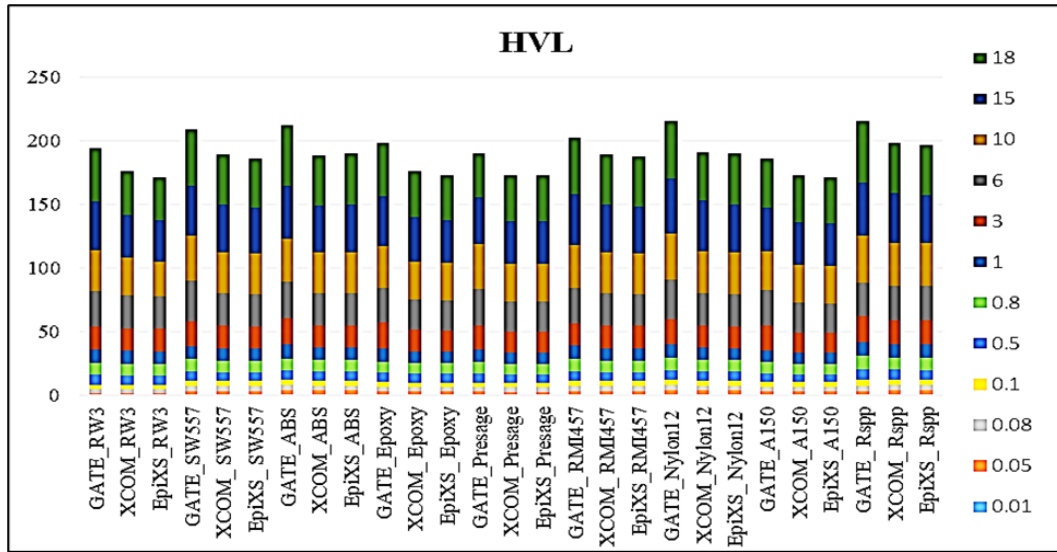


**Figure 2.** HVL values according to energy variation

Table 6 presents the  $\Sigma R$  values of the selected materials. These values were obtained using empirical formulas from equations 4, 5, and 6, as well as MCNP5 Monte Carlo simulation, MRCsC, and Phy-X/PSD software programs. In the study conducted by Hila et al. [11], they numerically generated fast neutron mass removal cross-sections ( $\Sigma_R/\rho$ ,  $\text{cm}^2/\text{g}$ ) based on ENDF/B-VIII.0 using a sliced spherical shell Monte Carlo model under different neutron source spectra. Using the generated  $\Sigma_R/\rho$  values in this study,  $\Sigma_R$  values for various materials were determined. For effective neutron shielding, materials with high  $\Sigma_R$  values are desired. According to Table 6, the material with the highest  $\Sigma R$  value is Nylon<sub>12</sub> ( $0.131 \text{ cm}^{-1}$ ). Generally, as the content of low Z elements increases, the  $\Sigma R$  value also increases. In Table 6, the material with the highest hydrogen (H) content is Nylon<sub>12</sub>. Therefore, it is thought that the highest  $\Sigma_R$  value is observed in this material. The lowest  $\Sigma R$  value was observed in Rspp ( $0.048 \text{ cm}^{-1}$ ). This is due to the absence of hydrogen (H) content in

this material. This is because the fast neutron mass removal cross-section of hydrogen is much higher than that of many other elements. In their study, Elwahab et al. [27] stated that hydrogen atoms play a significant role in the slowing-down mechanisms of fast neutrons, implying that the slowing-down process would be maximized when the hydrogen atoms are at their maximum. After Nylon<sub>12</sub> material, the best  $\Sigma R$  values are found in the following order: Presage, ABS, A<sub>150</sub>, SW<sub>555</sub>, RMI<sub>457</sub>, RW<sub>3</sub>, epoxy, and Rspp, respectively. The lower  $\Sigma R$  value of Rspp compared to other materials is thought to be due to the absence of hydrogen element in its structure. The  $\Sigma R$  values of materials such as Nylon<sub>12</sub>, presage, ABS, A<sub>150</sub>, SW<sub>555</sub>, RMI<sub>457</sub>, RW<sub>3</sub> and epoxy were found to be close to the  $\Sigma R$  values of paraffin, water, Hematite-serpentine, and concrete. It was observed that the  $\Sigma R$  values obtained for epoxy using the MRCsC program are larger than those of presage, water, concrete, and Hematite-serpentine.

**Table 6.** Values of  $\Sigma R$  for different calculation

Materials	MNCPS	MRCsC	$\Sigma R$ (cm <sup>-1</sup> )		Experiments
			Phy-X/PSD	Estimation using $\Sigma R/\rho$ of elements	
RW <sub>3</sub>	0.084	0.106	0.095	0.096	-
SW <sub>557</sub>	0.085	0.108	0.095	0.094	-
ABS	0.088	0.113	0.097	0.098	-
Epoxy	0.081	0.103	0.091	0.090	-
Presage	0.095	0.119	0.106	0.105	-
RMI <sub>457</sub>	0.085	0.107	0.094	0.094	-
Nylon <sub>12</sub>	0.105	0.131	0.113	0.114	-
A <sub>150</sub>	0.097	0.111	0.117	0.107	-
RspP	0.038	0.048	0.046	0.047	-
H <sub>2</sub> O	0.100	0.110	0.103	0.103	-
Paraffin, C <sub>25</sub> H <sub>52</sub>	0.119	0.141	0.122	0.122	0.109 [29]
Concrete, Dry	0.086	0.102	0.093	0.085	0.087 [29]
Fluoroethene, C <sub>2</sub> F <sub>3</sub> Cl	0.080	0.096	0.078	0.079	0.075 [29]
Perfluoroheptane, C <sub>7</sub> F <sub>16</sub>	0.071	0.080	0.067	0.068	0.070 [29]
Hematite–serpentine [28]	0.101	0.103	0.103	0.100	-

#### 4. Conclusion and Suggestions

In this study, the LAC, MAC, HVL, MFP, and  $\Sigma R$  values of various water-equivalent materials, especially those used for quality control in radiotherapy, were obtained using Monte Carlo simulation, MRCsC, Phy-X/PSD, EpiXS computer programs, and XCOM. For daily and weekly quality control procedures in radiotherapy, RW<sub>3</sub> exhibited better MAC, LAC, HVL, and MFP values compared to other materials. However, upon examining the  $\Sigma R$  values, it was found that Nylon<sub>12</sub> is the best material

for neutron shielding. The results obtained from this study can serve as a database for researchers and designers working on both photon and neutron shielding. Additionally, these materials offer advantages over existing shielding materials, such as low thickness, lightweight, durability, and non-toxicity. Moreover, these materials can be used in various applications, including radiation therapy rooms, the transportation of chemical isotopes, and other diverse radiation sources.

#### Statement of Research and Publication Ethics

The study is complied with research and publication ethics.

#### References

- [1] M. G. Dong, M. I. Sayyed, G. Lakshminarayana, M. Ç. Ersundu, A. E. Ersundu, P. Nayar, and M.A. Mahdi, "Investigation of gamma radiation shielding properties of lithium zinc bismuth borate glasses using XCOM program and MCNP5 code", *Journal of Non-Crystalline Solids*, vol. 468, pp. 12-6, 2017.
- [2] M. Schulc, M. Kostal, E. Novak, R. Kubín, and J. Simon, "Application of 252Cf neutron source for precise nuclear data experiments", *Applied Radiation and Isotopes*, vol. 151, pp. 187–195, 2019.
- [3] F. C. Hila, C. A. M. Dingle, A. Asuncion-Astronomo, C. V. Balderas, M. L. Grande, K. M. D. Romallosa, N. R. D. Guillermo, "Evaluation of time-dependent strengths of californium neutron sources by decay of 252Cf, 250Cf, and 248Cm: uncertainties by Monte Carlo method", *Applied Radiation and Isotopes*, vol. 167, 2021a.
- [4] J. Biau, E. Chautard, P. Verrelle, and M. Dutreix, "Altering DNA repair to improve radiation therapy: specific and multiple pathway targeting", *Frontiers in oncology*, vol. 9, pp.1009, 2019.
- [5] R. E. Stoller, "Radiation damage correlation. In: Comprehensive Nuclear Materials", *Elsevier*, pp. 456–467, 2020.

- [6] M. K. A. Roslan, M. Ismail, A. B. H. Kueh, and M. R. M. Zin, “High-density concrete: exploring Ferro boron effects in neutron and gamma radiation shielding”, *Construction and Building Materials*, vol. 215, pp.718-725, 2019.
- [7] M. G. Dong, X. X. Xue, Y. Elmahroug, M. I. Sayyed, and M. H. M. Zaid, “Investigation of shielding parameters of some boron containing resources for gamma ray and fast neutron”, *Results in Physics*, vol. 13, pp. 1-7, 2019.
- [8] C. V. More, R. R. Bhosale, and P. P. Pawar, “Detection of new polymer materials as gamma-ray-shielding materials”, *Radiation Effects and Defects in Solids*, vol. 172, pp.469-484, 2017.
- [9] M. Büyükyıldız, M. A. Taşdelen, Y. Karabul, M. Çağlar, O. İçelli, and E. Boydaş, “Measurement of photon interaction parameters of high-performance polymers and their composites”, *Radiation Effects and Defects in Solids*, vol. 173, pp.474-488, 2018.
- [10] N. R. Abd Elwahab, N. Helal, T. Mohamed, F. Shahin, and F. M. Ali, “New shielding composite paste for mixed fields of fast neutrons and gamma rays”, *Materials Chemistry and Physics*, vol. 233, pp.249-253, 2019.
- [11] F. C. Hila, J. F. M. Jecong, C. A. M., Dingle, A. J. Asuncion-Astronomo, C. V. Balderas, J. A. Sagum, and N. R. D. Guillermo, “ENDF/B-VIII. 0-based fast neutron removal cross sections database in  $Z= 1$  to 92 generated via multi-layered spherical geometry”, *Radiation Physics and Chemistry*, vol. 206, p.110770, 2023.
- [12] O. Agar, “Study on gamma ray shielding performance of concretes doped with natural sepiolite mineral” *Radiochim. Acta*, vol. 106, pp. 1009–16, 2018.
- [13] H. O. Tekin, E. Kavaz, A. Papachristodoulou, M. Kamislioglu, O. Agar, E. A. Guclu, O. Kilicoglu, and M. I. Sayyed, “Characterization of  $\text{SiO}_2\text{-PbO-CdO-Ga}_2\text{O}_3$  glasses for comprehensive nuclear shielding performance: Alpha, proton, gamma, neutron radiation”, *Ceramics International*, vol. 45, pp.19206-19222, 2019.
- [14] M. I. Sayyed, A. Kumar, H. O. Tekin, R. Kaur, M. Singh, O. Agar, and M. U. Khandaker, “Evaluation of gamma-ray and neutron shielding features of heavy metals doped  $\text{Bi}_2\text{O}_3\text{-BaO-Na}_2\text{O-MgO-B}_2\text{O}_3$  glass systems”, *Progress in Nuclear Energy*, vol. 118, p.103118, 2020.
- [15] Y. Al-Hadeethi, and M. I. Sayyed, “Radiation attenuation properties of  $\text{Bi}_2\text{O}_3\text{-Na}_2\text{O-V}_2\text{O}_5\text{-TiO}_2\text{-TeO}_2$  glass system using Phy-X/PSD software” *Ceramics international*, vol. 46, pp.4795-4800, 2020.
- [16] L. K. Zoller, “Fast-neutron removal cross sections”, *Nucleonics*, vol. 22, 1964.
- [17] M.G. El-Samrah, A. M. El-Mohandes, A. M. El-Khayatt, and S. E. Chidiac, “MRCsC: A user-friendly software for predicting shielding effectiveness against fast neutrons”, *Radiation Physics and Chemistry*, vol. 182, 2021.
- [18] F. C. Hila, A. Asuncion-Astronomo, C. A. M. Dingle, J. F. M. Jecong, A. M. V. Javier-Hila, M. B. Z. Gili, C. V. Balderas, G. E. P. Lopez, N. R. D. Guillermo, and A. V. Amorsolo Jr, “EpiXS: A Windows-based program for photon attenuation, dosimetry and shielding based on EPICS2017 (ENDF/B-VIII) and EPDL97 (ENDF/B-VI. 8)”, *Radiation Physics and Chemistry*, vol. 182, 2021b.
- [19] Şakar, E., Özpolat, Ö.F., Alım, B., Sayyed, M.I. and Kurudirek, M., 2020. Phy-X/PSD: development of a user-friendly online software for calculation of parameters relevant to radiation shielding and dosimetry”, *Radiation Physics and Chemistry*, 166, p.108496.
- [20] N. Ade, D. Eeden, and F. C. P. van, Plessis, “Characterization of Nylon-12 as a water-equivalent solid phantom material for dosimetric measurements in therapeutic photon and electron beams”, *Applied Radiation and Isotopes*, vol. 155, p.108919, 2020.
- [21] F. Araki, “Dosimetric properties of a Solid Water High Equivalency (SW557) phantom for megavoltage photon beams”, *Physica Medica*, vol. 39, pp. 132–136, 2017.
- [22] R. Kumar, S. D. Sharma, S. Desphande, Y. Ghadi, V. S. Shaiju, H. I. Amols, and Y. S. Mayya, “Acrylonitrile Butadiene Styrene (ABS) plastic-based low-cost tissue equivalent phantom for verification dosimetry in IMRT”, *Journal of Applied Clinical Medical Physics*, vol. 11, no. 1, pp. 24-32, 2009.
- [23] V. P. Singh, N. M. Badiger, and N. Kucuk, “Assessment of methods for estimation of effective atomic numbers of common human organ and tissue substitutes: waxes, plastics and polymers”, *Radioprotection*, vol 49, no. 2, pp.155-21, 2014.

- [24] S. Brown, A. Venning, Y. De Deene, P. Vial, L. Oliver, J. Adamovics, and C. Baldock, “Radiological properties of the PRESAGE and PAGAT polymer dosimeters”, *Applied Radiation and Isotopes*, vol 66, pp. 1970–74, 2008.
- [25] T. Şahmaran, and A. Kaşkaş, “Comparisons of various water-equivalent materials with water phantom using the Geant4/GATE simulation program”, *International Journal of Radiation Research*, vol 20, no. 3, pp.709-714, 2022.
- [26] M. M. Mohd Yusof, R. Hashim, A. A. Tajuddin, S. Bauk, and O. Sulaiman, “Characterization of Rhizophora spp. particleboards as phantom for photon beams”, *Ind. Crop. Prod.*, vol. 965, 467-474, 2017.
- [27] N. R. Abd Elwahab, N. Helal, T. Mohamed, F. Shahin, and F. M. Ali, “Calculation of Fast neutron Removal Cross-section and Gamma ray Attenuation for New composite Paste Shields”, *Interciencias Journal*, vol 44, no. 8, 2019.
- [28] A. M. S. Issa, K. Ashok, M. I. Sayyed, M. G. Dong, and Y. Elmahroug, “Mechanical and gamma-ray shielding properties of TeO<sub>2</sub>-ZnO-NiO glasses”, *Mater. Chem. Phys.*, vol. 212, pp. 12-20, 2018.
- [29] G. T. Chapman, and C. T. Storrs, Effective Neutron Removal Cross Sections for Shielding. USAEC Report ORNL-1843 (AECD-3978). Oak Ridge National Laboratory, Oak Ridge, Tennessee, 1995.